Research on Electric Drive Control Method Based on Parallel Computing

Lin-ze Gao(✉)

Guilin University of Electronic Technology, Guilin 536000, China
gaolz20@126.com

Abstract. In order to solve the problems of low control accuracy and poor stability of traditional electric drive control methods, a parallel computing based electric drive control method is proposed. According to the selected motor parameters, the transmission point with the maximum power or the strongest mechanical rigidity is selected as the main node, so that the parameters are equal to the load rate of the load distribution motor, and the load distribution is completed by parallel calculation; the air gap magnetic field is generated inside the motor, and the electromagnetic thrust is generated under the interaction with the excitation magnetic field generated by the permanent magnet by using the concepts of coordinate transformation and space vector Force is used to push the motor to move synchronously and linearly at the same speed to complete the motor vector control and the electrical drive control based on parallel computing. The experimental results show that the control accuracy of the proposed method is high and the operation is stable. It can effectively reduce the position tracking error and improve the control accuracy.

Keywords: Parallel computing · Electric drive · Control method · Motor parameters · Load rate · Air gap magnetic field

1 Introduction

Parallel computing is also known as parallel computing, as opposed to serial computing. It is an algorithm that can execute multiple instructions at a time. Its purpose is to improve the computing speed, and to solve large and complex computing problems by expanding the problem solving scale [1]. Parallel computing refers to the process of using multiple computing resources to solve computing problems at the same time, and is an effective means to improve the computing speed and processing power of computer systems. Its basic idea is to solve the same problem with multiple processors, the problem to be solved is decomposed into several parts, each part is calculated by an independent processor in parallel [2–4]. A parallel computing system can be a specially designed supercomputer containing multiple processors, or it can be a cluster of several independent computers interconnected in a certain way. Complete the data processing through the parallel computing cluster, and then return the processing results to the user.

Parallel computing can be divided into time parallel and space parallel. Time parallel refers to assembly line technology. For example, the steps of food production in the factory are divided into: cleaning: washing the food. Disinfection: disinfect the

S. Liu and L. Xia (Eds.): ADHIP 2020, LNICST 348, pp. 180–191, 2021.
https://doi.org/10.1007/978-3-030-67874-6_17

food. Cutting: Cut food into small pieces. Packaging: pack the food in the packaging bag. If the assembly line is not used, after a food completes the above four steps, the next food is processed, which takes a long time and affects efficiency. However, using pipeline technology, multiple foods can be processed simultaneously. In parallel algorithm, time is parallel, and two or more operations are started at the same time to improve the computing performance. Spatial parallelism refers to the concurrent execution of computation by multiple processors, that is, connecting more than two processors through the network to simultaneously compute different parts of the same task, or a large-scale problem that cannot be solved by a single processor.

In parallel computing, computing problems usually show the following characteristics:

1. Separate work into discrete parts, which helps to solve at the same time;
2. Execute multiple program instructions at any time and in time;
3. Solve under multiple computing resources.

The problem takes less time than a single computing resource. Parallel computing science mainly studies spatial parallel problems. From the perspective of programmers and algorithm designers, parallel computing can be divided into data parallel and task parallel. Generally speaking, data parallelism is mainly to resolve a large task into the same sub tasks, which is easier to handle than task parallelism. Spatial parallelism has led to the creation of two types of parallel machines. According to flynn, it is divided into: single instruction stream multiple data streams and multiple instruction streams multiple data streams. Commonly used serial machines are also called single instruction streams and single data streams. MIMD machines can be divided into the following five common categories: parallel vector processors, symmetric multiprocessors, large-scale parallel processors, workstation clusters, and distributed shared storage processors. Parallel computers connect each processor or processor by network. Generally, there are several ways as follows: a kind of network with fixed connection between processing units. During program execution, the point-to-point connection remains unchanged; typical static networks include one-dimensional linear array, two-dimensional mesh, tree connection, hypercube network, cubic ring, shuffle switching network, butterfly network, etc.

In recent years, with the development of motor manufacturing technology and power electronics technology, and the increasingly mature motor control technology, its comprehensive performance has been greatly improved [5]. In foreign literature, the electric load simulation research for testing motor and electric power rotating load capacity is proposed. At present, many foreign scholars study a load motor control method by means of the mechanical load simulation experimental platform of the drive motor load motor to realize the simulation of the dynamic mechanical load of the experimental platform, and finally realize the verification and test of various advanced control algorithms; it can also test the performance of the motor, electric drive system and driver in the experimental platform. Since the 1960s, there has been research work in this area. Until today, electric drive control has been greatly developed, but there is still some room for improvement. The following research will use parallel computing in the original electric drive control method. It is optimized on the basis to improve the effect of electric drive control.

2 Electric Drive Control Method Based on Parallel Computing

2.1 Load Distribution Based on Parallel Computing

The simple speed chain control can not meet the requirements of transmission control, so it needs to use different load distribution methods to control. The basic principle of load distribution is that the load rate of each transmission motor is the same, and each motor should distribute the overall load according to the load rate.

The load factor α of the motor has the following relationship:

$$\alpha = \frac{Q_a}{Q_{ab}} \tag{1}$$

In the formula, Q_a represents the actual power of the a motor, and Q_{ab} represents the rated power of the a motor.

In formula (1), the motor power represents the actual load, which can also represent the parameters of the actual load as well as the current and torque. The torque is selected as the parameter, and the load distribution of torque is as follows:

$$Y_a = \frac{Y_{ab} \times Y}{\sum_{a=1}^{n} Y_{ab}} \tag{2}$$

In the formula, Y_a is the expected torque of the a th motor; Y_{ab} is the rated torque of the a th motor; Y is the total torque of the load; n is the number of motors participating in the load distribution.

In summary, the load distribution is based on the selected parameters, so that each parameter is equal to the motor load rate of the load distribution. There are many different distribution methods for load distribution, which can be summarized as two types of control methods: load distribution based on speed control and load distribution based on torque control. Select one of the inverters as the main node for load distribution. Generally, the transmission point with the largest power or the strongest mechanical rigidity is selected as the main node. Turn on the speed control mode and hang it on the speed chain to form the speed chain with other inverters [6–8]. Then load distribution is carried out according to the actual distribution situation.

The first case is the remaining point of felt ring, the main node is set as grid driven roller, and the torque is set to 1, the torque of the remaining nodes is given, and then given according to the actual power of the motor. For example, the short former is 0.7 and the vacuum roll is 0.5, then the relationship between the torque setting of the short former and the mesh drive roller and the mesh drive roller is 0.7: 0.5: 1, that is, all the loads are distributed to each point. The second case is the two-point contact load distribution, such as pressing the upper and lower rollers. Taking the press lower roll as the main point, the moment value of the press lower roll multiplied by a coefficient is directly taken as the given moment of the press upper roll. This coefficient can be calculated according to the actual situation. The flow chart is as follows:

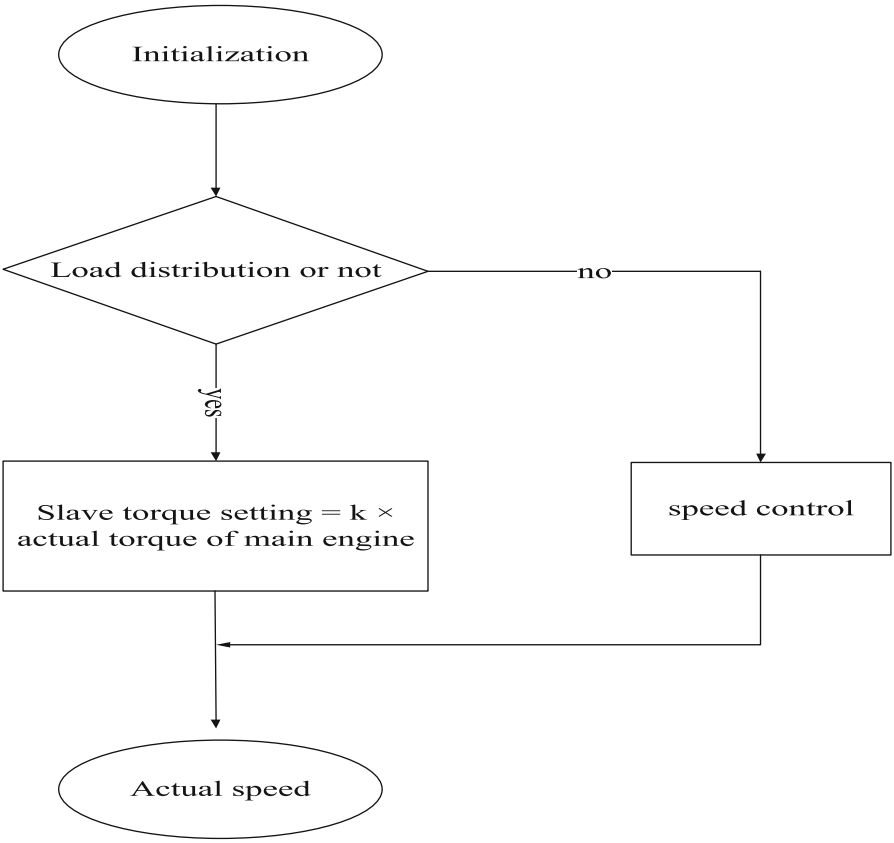

Fig. 1. Flow chart of load distribution program structure

In the Fig. 1, *K* is a constant. When designing the software for load distribution, you need to pay attention to the following issues: First, it cannot be disconnected from the main speed chain. The load distribution can only be hung on the main speed chain as a subsystem. The load distribution process cannot affect the other motors. Speed and status [9–11]. Second, the load distribution should consider the very short case, such as the runaway caused by the loose contact surface, and the load should be limited. Third, according to the actual production, some points in the paper introduction process are open, so it is necessary to install conversion device. For example, pressure sensor is used for conversion, speed chain control is used when opening, and load distribution is changed when the pressure reaches.

2.2 Motor Vector Control

In structure, the motor can be regarded as a rotating motor that splits along the radial direction and expands the circumference into a straight line. It changes from the stator of the rotating motor to the primary one, from the rotor to the secondary one. The moving part of the linear motor is defined as the motor, and the fixed part is defined as the stator as shown in Fig. 2:

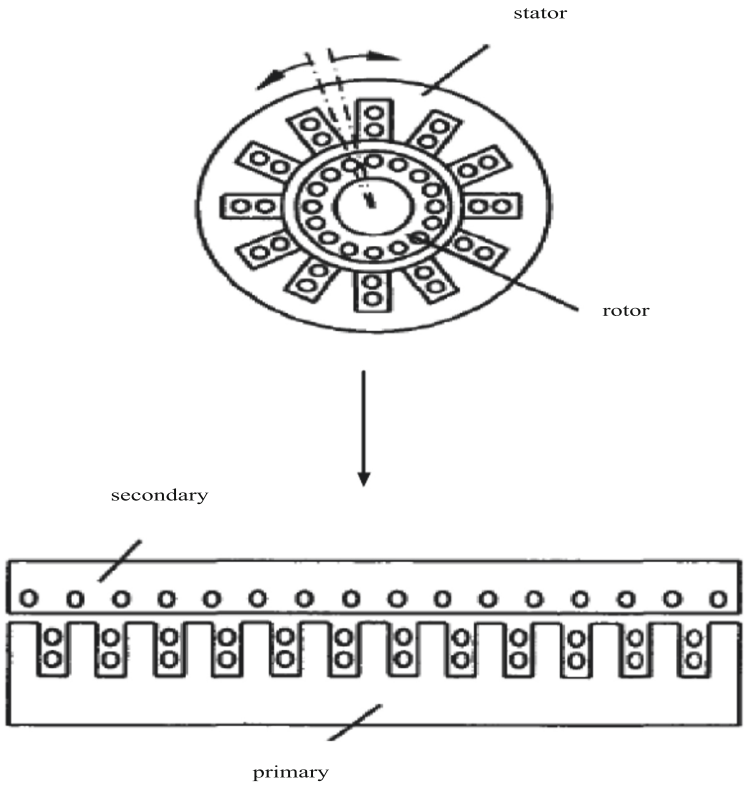

Fig. 2. Schematic diagram of rotating motor evolving into linear motor

From the structural point of view, the linear motors are mainly disc type, flat type, arc type and cylindrical type. For flat linear motors, if the primary is installed only on the secondary side, it is unilateral linear Motor, it will have a relatively large normal force; If the primary is installed on both sides of the secondary (armature winding part is installed on both sides of the pole) or the secondary is installed on both sides of the primary (armature winding part is installed on both sides) In the middle of the magnetic pole), it is a bilateral linear motor. There are short primary and short secondary structures for unilateral and bilateral linear motors. Among them, the operation cost and manufacturing cost of the short primary linear motor are relatively low, so in most cases, the short primary linear motor is used [12, 13]. The following research focuses

on the electric drive control of the short primary bilateral flat AC permanent magnet synchronous linear motor.

For the AC permanent magnet synchronous linear motor, a three-phase symmetrical and time-varying sinusoidal current is input into the winding, and an air gap magnetic field is generated inside the motor, as shown in Fig. 3:

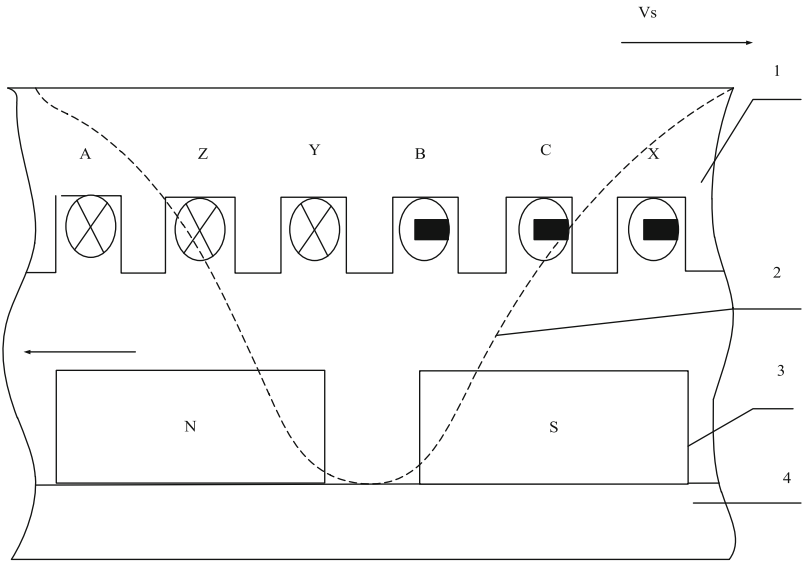

Fig. 3. Working principle of permanent magnet synchronous linear motor

In Fig. 3, 1 represents the mover and primary; 2 represents the traveling wave magnetic field; 3 represents the permanent magnet; 4 represents the stator and secondary. If the longitudinal side effect is ignored, the air gap magnetic field is also sinusoidal and moves along a straight line according to the phase sequence a, B and C, which is called traveling wave magnetic field. Under its interaction with the excitation magnetic field generated by the permanent magnet, an electromagnetic thrust is generated, which pushes the motor mover to perform synchronous linear motion at the same speed as it. The speed of the traveling wave magnetic field is:

$$B_\beta = 2f\beta \tag{3}$$

In the formula, B_β is the traveling wave magnetic field speed; f is the three-phase alternating current frequency; β is the magnetic pole center distance of the permanent magnet synchronous motor.

Under certain assumptions, the concepts of coordinate transformation and space vector can be used to simplify and calculate the nonlinear system with multi input and multi output, time-varying and multi variable coupling. It is assumed that: the magnetic circuit is linear, ignoring hysteresis, eddy current, remanence and saturation effects; the winding magnetic potential and air gap magnetic density are sinusoidal distribution, and ignoring spatial harmonics.

From the point of view of motor structure, linear motor can be considered as a kind of radial evolution of rotating motor. The following assumes that the permanent magnet synchronous linear motor is a rotating motor, and imagines its magnetic field as a rotating space magnetic field, so as to complete the Vector control. Three reference coordinate systems are commonly used in the analysis and establishment of their mathematical models, which are $q-w-e$ coordinate system, $\partial-\wp$ coordinate system and $x-y$ coordinate system, of which $q-w-e$ coordinate system and $\partial-\wp$ coordinate system are armature static coordinate systems, and $x-y$ coordinate system is space rotation dynamic coordinate system.

$q-w-e$ three phase coordinate system is composed of three-phase windings A, B and C of the armature, and the corresponding axes are q, w and e with an electric angle of 120° different from each other, forming a plane vector, as shown in Fig. 4:

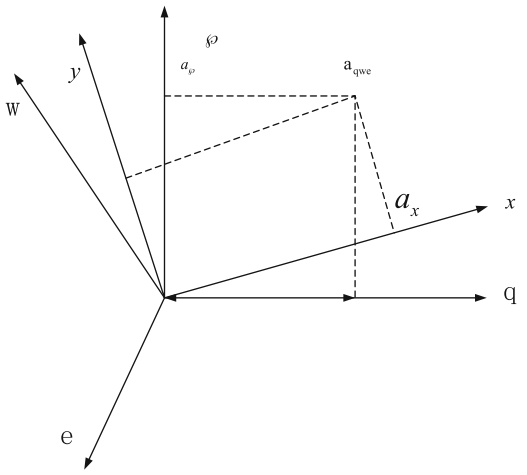

Fig. 4. Coordinate systems of AC permanent magnet synchronous motor

From the mathematical point of view, the plane vector can be described by using a rectangular coordinate system, so in the motor coordinate system, set $\partial-\wp$ rectangular coordinate system to simplify the calculation; where ∂ and q axis coincide, $\wp$ is 90° ahead of e axis.

The space current vector in $\partial-\wp$ coordinate system is:

$$\vec{a}_{qwe}=a_{\partial}+a_{\wp}b=\frac{2(a_q+a_wb^{120?}+a_eb^{240?})}{3} \tag{4}$$

In the formula, the current components in the $\partial-\wp$ rectangular coordinate system where a_{∂} and $a_{\wp}$ are stationary; a_q, a_w, and a_e are the current values input in the $q-w-e$ three-phase coordinate system. With the movement of the motor, the space magnetic field rotates correspondingly with $\vec{a}_{qwe}$. Imagine a rotating two-phase rectangular coordinate system $x-y$, which rotates at the same angular velocity as $\vec{a}_{qwe}$, so

the current can be divided into thrust current a_y and excitation current a_x in the $x-y$ coordinate system. If a_y and a_x are controlled separately, it can be completed Current decoupling control. The position angle μ of the $x-y$ coordinate system relative to the $\partial-\wp$ coordinate system is:

$$\mu = \mathrm{mod}\left(\frac{u}{2\beta}\right) * (2\pi) + \mu_0 \tag{5}$$

In the formula, u is the displacement; μ_0 is the initial position angle; mod is the modulus operator.

The changing process of $q-w-e$ to $\partial-\wp$ coordinate system is:

$$Z_{\mathrm{qwe}-\partial\wp} = \frac{2}{3}\begin{bmatrix} 1 & -\frac{1}{2} & -\frac{1}{2} \\ 0 & \frac{\sqrt{3}}{2} & \frac{\sqrt{3}}{2} \end{bmatrix} \tag{6}$$

or

$$Z_{\mathrm{qwe}-\partial\wp} = \frac{2}{3}\begin{bmatrix} 1 & 0 & \frac{1}{2} \\ -\frac{1}{2} & \frac{\sqrt{3}}{2} & -\frac{\sqrt{3}}{2} \\ -\frac{1}{2} & \frac{1}{2} & \frac{1}{2} \end{bmatrix} \tag{7}$$

Changes from $\partial-\wp$ to $q-w-e$ coordinate system:

$$Z_{\partial\wp-\mathrm{qwe}} = \frac{2}{3}\begin{bmatrix} 1 & 0 \\ -\frac{1}{2} & \frac{\sqrt{3}}{2} \\ -\frac{1}{2} & -\frac{\sqrt{3}}{2} \end{bmatrix} \tag{8}$$

or

$$Z_{\partial\wp-\mathrm{qwe}} = \frac{2}{3}\begin{bmatrix} 1 & 0 & \frac{1}{2} \\ -\frac{1}{2} & \frac{\sqrt{3}}{2} & \frac{1}{2} \\ -\frac{1}{2} & -\frac{\sqrt{3}}{2} & \frac{1}{2} \end{bmatrix} \tag{9}$$

Through the above process, the current is converted from the three-phase $q-w-e$ coordinate system to the right-angle $x-y$ coordinate system to realize the decoupling control process, and the study of the electric drive control method based on parallel calculation is completed.

3 Experimental Analysis

3.1 Experimental Environment

In order to verify the effectiveness of the proposed method, simulation experiments are carried out. The experiment was carried out on MATLAB platform, using Windows 10

system, running memory of 8 GB. In this experimental environment, a comparative experiment is designed to verify the effectiveness of the proposed method. The composition of the experimental platform is shown in Table 1:

Table 1. Main components of the experimental platform

Name	Model	Quantity	Performance parameter
Motion controller + adapter board	Turbo PMAC2 Clipper + DTC-8B	1 + 1	DSP56303 4 axis board
Linear encoder	RGH22Y	2	Resolution is 0.1μm Normal reading Allowable speed is 4 m/s
Driver	D1 MD-36-S	2	Frequency Range 47 ~ 63 Hz
X axis guide rail + slider	QHH15H1026Z-1082 + QH15	2 + 4	Self-lubricating
Y axis guide rail + slider	QHH20H1026Z-5068 + QH20	2 + 4	Self-lubricating
X axis permanent magnet synchronous linear motor	LMCB6	1	Stroke 750 mm
Y-axis permanent magnet synchronous linear motor	LMCC8	1	Stroke 1000 mm
Limit switch	EE-SX674	6	–

3.2 Experimental Parameters

When the load of the CNC platform is set to 17 kg and the external environment is relatively constant, the parameters of the position ring of x-axis linear motor and y-axis linear motor are as follows:

Table 2. Parameter settings

Motor shaft	X axis	Y axis
load	17 kg	48 kg
Kp	122	103
Ki	52	31
Kd	185	147
Kvff	1650	1950
Kaff	0	0

3.3 Experimental Scheme

In order to verify the rationality of the proposed method, the KP parameters of the proposed method and the traditional method are compared, and the stability of the proposed method and the traditional method in electrical drive control is analyzed. In order to ensure the credibility of the experiment, the experimental results are obtained through many experimental iterations and analysis.

3.4 Analysis of Experimental Results

3.4.1 Control Accuracy Analysis by Different Methods

In order to verify the comprehensive effectiveness of the proposed method, experimental analysis of the proposed method and traditional methods to adjust the Kp parameter, the experimental results are shown in Fig. 5:

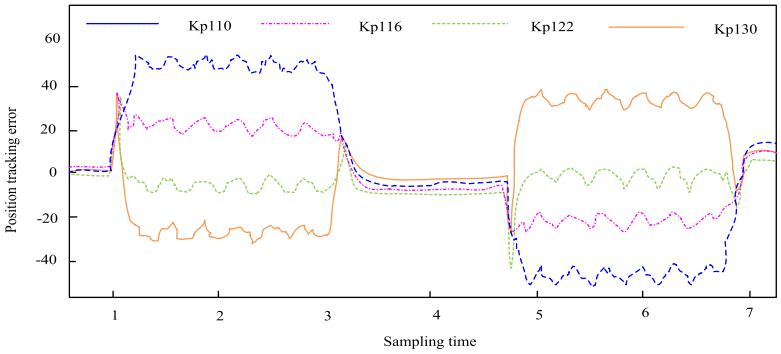

(a) Proposed control method

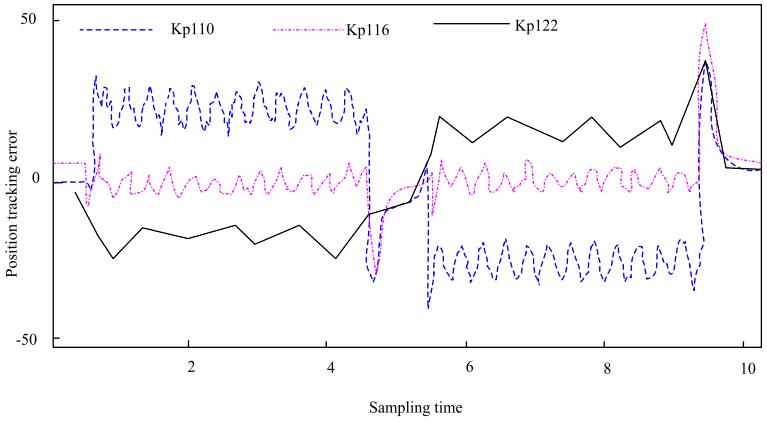

(b) Original control method

Fig. 5. Comparison of the effects of adjusting Kp parameters by different methods

Analysis of Fig. 5 shows that the proposed method uses the X-axis parameters in Table 2 under a load of 17 kg, and makes Kp equal to the errors obtained by 110, 116, 122, and 130, respectively, as shown in Figure (a). With the increase of Kp, the trend of the error changes firstly decreases in the positive direction and then increases in the negative direction. Under this control method, the optimal Kp = 122, and the position tracking error at this time is (–8, 9) μm.

Adopt the original control method, adopt the x-axis parameters in Table 2, and make KP be the error of 110, 116 and 122 respectively, as shown in figure (b). The trend of error change is also with the increase of KP, which first decreases in the positive direction and then increases in the negative direction. Under the traditional control method, the optimal KP = 116, at this time, the position tracking error is (–7,10) μ m, while when KP = 122, the position tracking error is (–24,22) μ M. In contrast, the proposed method has smaller tracking error and higher accuracy.

3.4.2 Control Stability Analysis by Different Methods

In order to further verify the scientific validity of the proposed method, the stability analysis of the proposed method and the traditional method in the electric drive control is analyzed in the experiment, and the experimental results are shown in Fig. 6:

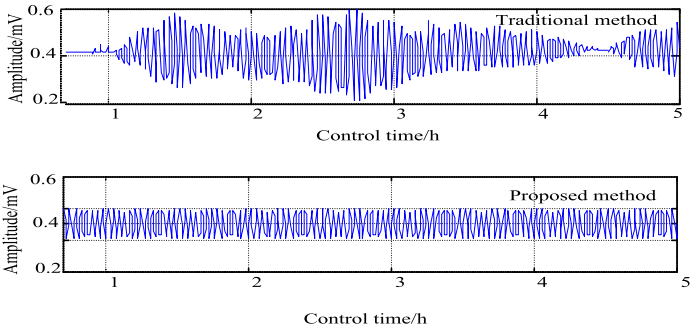

Fig. 6. Comparison of control stability with different methods

Analysis of Fig. 6 shows that under the same experimental environment, the control stability of the two methods is somewhat different. Among them, the control stability of the proposed method is always between 0.35 mV and 0.45 mV, which is better and more stable; while the control stability of the traditional method is more volatile. In contrast, the proposed method has good control stability and is feasible.

4 Conclusion

The research of the electric drive control method based on parallel computing is put forward. Through the selection of motor parameters and effective load distribution, the effective control of electric drive is realized.

Experimental results show that the proposed method can effectively improve the control accuracy and has good stability. However, due to the short research time, there are still some imperfections that need to be optimized in subsequent studies.

References

1. Shaoyan, H.E., Chunhui, W.U., Jianjun, T.I.A.N.: Review of the current transducer techniques. Electric Drive **48**(01), 65–75 (2018)
2. Le, H.A.N.: The application of plc in the integration of electric power drive. Telecom Power Technol. **36**(04), 89–90 (2019)
3. Xingtian, F., Huihui, H., Rong, C.: Teaching reform of engineering quality for automatic control system of electric drive. J. Electrical Electronic Educ. **40**(03), 47–49 (2018)
4. Yan, L.I.: Research and application of single chip microcomputer in electric drive control system. Telecom Power Technol. **35**(02), 169–170 (2018)
5. Fuzhong, W., Yuanyuan, L., Sumin, H., et al.: Status assessment of mine hoist electric drive system based on fuzzy synthetic evaluation. Power System Protect. Control **47**(09), 166–172 (2019)
6. Liu, S., Lu, M., Li, H., et al.: Prediction of gene expression patterns with generalized linear regression model. Front. Genetics **10**, 120 (2019)
7. Yue, P.: Selection of Fan and pump motor and electric drive system. Moder Archit. Electric **9**(04), 13–16 (2018)
8. Yuening, J., Hongguang, J., Ming, L.: CFD numerical simulation of unmanned aerial vehicle based on multi-core parallel computation. Comput. Eng. Appl. 54 (07), 221–225 (2018)
9. Liu, S., Liu, G., Zhou, H.: A robust parallel object tracking method for illumination variations. Mobile Netwk. Appl. **24**(1), 5–17 (2019)
10. Yaning, Y.: Unmanned aerial vehicle trajectory control simulation based on gpu parallel algorithm. Comput. Simul. **36**(03), 69–72 (2019)
11. Ying, C.: The construction and development of electric drive control training room in higher vocational colleges. Liaoning Higher Vocational Techn. Inst. J. **20**(03), 78–80 (2018)
12. Liu, S., Liu, D., Srivastava, G., et al.: Overview and methods of correlation filter algorithms in object tracking. Complex Intell. Syst. (2020) https://doi.org/10.1007/s40747-020-00161-4
13. Lu, M., Liu, S.: Nucleosome positioning based on generalized relative entropy. Soft. Comput. **23**(19), 9175–9188 (2018). https://doi.org/10.1007/s00500-018-3602-2